Static and Time-Resolved Step-Scan Fourier Transform Infrared Investigations of the Photoreaction of Halorhodopsin from *Natronobacterium Pharaonis*: Consequences for Models of the Anion Translocation Mechanism

Christian Hackmann,* Jarmila Guijarro,* Igor Chizhov,† Martin Engelhard,† Christoph Rödig,* and Friedrich Siebert*

*Sektion Biophysik, Institut für Molekulare Medizin und Zellforschung, Albert-Ludwigs-Universität, D-79104 Freiburg; and †Max-Planck-Institut für Molekulare Physiologie, D-44227 Dortmund, Germany

ABSTRACT The molecular changes during the photoreaction of halorhodopsin from *Natronobacterium pharaonis* have been monitored by low-temperature static and by time-resolved step-scan Fourier transform infrared difference spectroscopy. In the low-temperature L spectrum anions only influence a band around 1650 cm^{-1}, tentatively assigned to the C=N stretch of the protonated Schiff base of L. The analysis of the time-resolved spectra allows to identify the four states: K, L_1, L_2, and O. Between L_1 and L_2, only the apoprotein undergoes alterations. The O state is characterized by an all-*trans* chromophore and by rather large amide I spectral changes. Because in our analysis the intermediate containing O is in equilibrium with a state indistinguishable from L_2, we are unable to identify an N-like state. At very high chloride concentrations (>5 M), we observe a branching of the photocycle from L_2 directly back to the dark state, and we provide evidence for direct back-isomerization from L_2. This branching leads to the reported reduction of transport activity at such high chloride concentrations. We interpret the L_1 to L_2 transition as an accessibility change of the anion from the extracellular to the cytosolic side, and the large amide I bands in O as an indication for opening of the cytosolic channel from the Schiff base toward the cytosolic surface and/or as indication for changes of the binding constant of the release site.

INTRODUCTION

In contrast to the light-driven proton pump bacteriorhodopsin, for which many details of the proton transfer and energy conversion mechanism are understood at a molecular level (Brown et al., 1998; Haupts et al., 1997), much less is known about the corresponding aspects of the related chloride pump halorhodopsin (Oesterhelt, 1995). Although quite a number of halorhodopsins have been identified (Mukohata et al., 1999), only those from *Halobacterium salinarum* (sHR) and *Natronobacterium pharaonis* (pHR) have been extensively studied. Bacteriorhodopsin and halorhodopsins show a surprising homology between their primary structures (Lanyi et al., 1990) with the exception of the key residues D85 and D96, which function in bacteriorhodopsin as proton acceptors and proton donors for de- and reprotonation of the Schiff base. In pHR, the corresponding sites are occupied by T126 (111) and A137 (122), respectively (the corresponding numbers of sHR are placed between parentheses). As expected from these replacements, the normal photocycle of halorhodopsins does not contain an intermediate with a deprotonated Schiff base (M-like state).

In a recently published structure of sHR, chloride in its binding site could be identified. It accepts hydrogen bonds from two water molecules and from a serine side chain. The chloride is close to the Schiff base, although in unfavorable position for hydrogen bonding (Kolbe et al., 2000). Together with data on the photocycle and studies of site-directed mutants a detailed model on the chloride transport mechanism has been developed. In addition, time-resolved electric measurements have correlated chloride transport steps with formation of intermediates (Kalaidzidis et al., 1998; Ludmann et al., 2000).

In previous investigations, the photocycles of sHR and pHR have been studied by time-resolved ultraviolet-visible (UV-vis) spectroscopy (Kalaidzidis et al., 1998; Ludmann et al., 2000; Scharf and Engelhard, 1994; Váró et al., 1995a,b,c), the latter results on pHR being at variance with the data on sHR. It appears that the main difference between the two pigments is the lack of accumulation of the O state in the latter system, probably because of kinetic reasons (Váró et al., 1995c). The capability of light adaptation represents another difference between the two systems, sHR containing ~50% all-*trans* retinal in the dark and 75% in white light, whereas pHR contains 85%, irrespective of the illumination condition (Váró et al., 1995a; Zimányi and Lanyi, 1997).

Information on molecular changes during the photocycle has been obtained by infrared difference spectroscopy (Bousché et al., 1991; Braiman et al., 1994; Rothschild et al., 1988; Rüdiger et al., 1995; Walter and Braiman, 1994) and by resonance Raman spectroscopy

Received for publication 7 August 2000 and in final form 11 April 2001.

Address reprint requests to Freidrich Siebert, Sektion für Biophysik, Institut für Molekulare medizin und Zellforschung, Albert-Ludwigs-Universität, D-79104 Freiburg, Germany. Tel.: 49-761-203-5396; Fax: 49-761-203-5399; E-mail: frisi@uni-freiburg.de.

0006-3495/01/07/394/13 $2.00

(Alshuth et al., 1985; Ames et al., 1992; Diller et al., 1987; Gerscher et al., 1997). These data clearly demonstrate the light-induced all-*trans* → 13-*cis* isomerization of the chromophore, based on band positions very similar to those of bacteriorhodopsin. Time-resolved FTIR investigations of sHR seem to indicate a very slow rise of L (300 μs) (Dioumaev and Braiman, 1997), at variance with the UV-vis data. In most models of the chloride transport mechanism it is assumed that the red-shifted O state, which can be accumulated in pHR, represents a state without bound chloride, i.e., a state in which the anion has been essentially released but not yet taken up. For pHR, a red-shifted dark state can be obtained by lowering the concentration of anions that are pumped, and a detailed analysis of the interdependence of pH, anion concentrations and absorption maximum has been performed (Scharf and Engelhard, 1994). Titrating this blue pHR (absorption maximum, 600 nm) with chloride a binding constant of 3 mM has been deduced.

Models on the anion transport mechanism have been recently developed, based on the structural data in the case of sHR (Kolbe et al., 2000) and on electrical and time-resolved UV-vis measurements in the case of pHR (Ludmann et al., 2000). Obviously, the models take into account many of the other published data of the two systems, especially also the similarities between bacteriorhodopsin and halorhodopsin. e.g., a single-site mutation in BR, i.e., D85T converts the proton pump into a chloride pump (Sasaki et al., 1995; Tittor et al., 1997). Furthermore, in the presence of azide, pHR can be converted into an efficient proton pump (Váró et al., 1996) with a photocycle similar to that of bacteriorhodopsin (Scharf and Engelhard, 1994), and sHR shows a two-photon-driven proton transport (Bamberg et al., 1993). Thus, it has been concluded that basic principles must be similar in these two ion pumps (Haupts et al., 1997; Kolbe et al., 2000). All models developed so far are based on assumptions which are not always unequivocally proven, and they make predictions which still await confirmation.

In order to contribute to the discussion on the anion pumping mechanisms, we report on time-resolved step-scan FTIR investigations with 30-ns time resolution of the photoreaction of pHR. This method, capable of detecting chromophore and protein molecular alterations (Uhmann et al., 1991; Weidlich and Siebert, 1993) has been successfully applied to the study of the light-induced molecular changes in bacteriorhodopsin (Rödig et al., 1999). pHR appears especially suitable for such studies, due to the fact that its greater stability allows to a large extent the variation of salts. We can identify the four different states, K, L_1, L_2, and O, and describe their characteristics with respect to chromophore and protein properties and their interconversion. In addition, we suggest a branching of the photocycle occurring at a very high NaCl concentration, which could explain the inhibition of chloride transport at such extreme conditions. The results are discussed within the framework of possible pumping mechanisms.

MATERIALS AND METHODS

Preparation of halorhodopsin samples

Halorhodopsin from *Natronobacterium pharaonis* was isolated according to Scharf and Engelhard (Scharf and Engelhard, 1994). Halorhodopsin expressed in *Escherichia coli* was prepared using the method of Hohenfeld et al. (1999). Reconstition of pHR into purple membrane lipids was performed following the procedure described in Losi et al. (Losi et al., 1999) .

Preparation of samples for infrared spectroscopy

Approximately 2 nmol of halorhodopsin reconstituted into lipids from *Halobacterium salinarum*, suspended in 100 μl buffer, 10 mM Tris/H_2SO_4 (pH 7), deposited onto a BaF_2 window, dried under nitrogen, and rehydrated with ~0.5 μl H_2O. Subsequently, the sample was sealed with a second window. Thus, the samples contained 1 μMol sulfate at an approximate concentration of 2 M. Depending on the experiment, the respective amount of salt was added in order to obtain the required anion concentration. It should be noted that the sample volume is very approximate. Therefore, the salt and buffer concentrations in the infrared samples may vary by ± 50%.

Time-resolved infrared measurements

Time-resolved step-scan FTIR measurements with 30-ns time resolution have been performed essentially as described (Rödig et al., 1999), with the exception that the fast (30-ns time resolution) and the slow (40-ns time resolution) measurements have been performed separately. With the fast setup, an ac-coupled amplifier has been used, limiting the covered time range to 100 μs. For sample excitation, a frequency-doubled Nd:YAG laser was used delivering 1.5 to 2 mJ to the sample with an approximate area of 1 cm^2. Spectral resolution is 8 cm^{-1}, eight signals have been averaged per interferogram sampling point, and four measurements are averaged. Measurements have been performed at room temperature. Before the infrared measurements, the same samples have been tested with respect to published data in a simple set-up for time-resolved UV-vis measurements.

Static low-temperature FTIR measurements

Static infrared difference spectra at 123 and 193 K have been obtained with a home-built cryostat inserted into a Bruker IFS 113v FTIR instrument, equipped with an MCT detector, essentially as described previously (Gerwert and Siebert, 1986). Spectral resolution is 2 cm^{-1}, and ~500 scans have been averaged before and after the illumination. For illumination, a slide projector connected to fiber optics has been used. To obtain the K state, the sample was illuminated with wavelengths between 490 and 550 nm at 123 K. To obtain the L state, the sample has been illuminated at 193 K with wavelengths longer than 610 nm.

Data evaluation of time-resolved infrared spectra

The time courses of the time-resolved spectra have been analyzed with the global fit program (MEXFIT)(Müller and Plesser, 1991) as described previously (Rödig et al., 1999). The resulting amplitude spectra have been converted into intermediate spectra, using the unidirectional reaction model without back-reactions (Chizhov et al., 1996), which has been successfully applied to the analysis of time-resolved infrared spectra of bacteriorhodop-

sin (Rödig et al., 1999). With this method, the derived intermediates generally are mixtures of pure states, the mixtures being in a fast equilibrium. As stated before, this kind of analysis provides a bias-free method of interpretation of time-resolved spectra, which does not suffer from the problem of free parameters. On the other hand, the intermediate spectra can be better described in molecular terms than the amplitude spectra because the latter are strongly influenced by the kinetic constants. We do not claim, however, that this reaction model represents the true path of the photocycle. In the analysis, there is generally the freedom for the sequence of the time constants. However, it turned out that only the series with increasing time constants provides reasonable and consistent intermediate spectra. In the following, we differentiate between intermediates, possibly being mixtures, and states representing pure states.

RESULTS

Low-temperature FTIR difference spectra

In Fig. 1, the low-temperature FTIR difference spectra of pHR in 500 mM NaCl are shown for comparison with the time-resolved spectra that are presented below. Although the spectra are very similar to earlier published data of sHR (Bousché et al., 1991; Rothschild et al., 1988) which reflects the homology of the two systems, a few remarks should be pointed out. At 123 K, the red-shifted K intermediate should be stabilized. However, no clear evidence for the ethylenic mode of the chromophore of this intermediate can be identified (assignments of chromophore bands are made on the basis of the corresponding bands of bacteriorhodopsin) (Fodor et al., 1988; Gerwert and Siebert, 1986; Smith et al., 1985). A band at 1514 cm^{-1}, detected in the corresponding spectrum of sHR (Rothschild et al., 1988), is not present in pHR. The band at 1500 cm^{-1} has a position too low for this assignment. For the correlation between the visible absorption maximum and the position of the ethylenic stretching mode of protonated retinylidene Schiff bases, see Heyde et al. (1971) and Ottolenghi (1980). It is striking that, in comparison to the spectrum obtained at 193 K, the band at 1525 cm^{-1}, mainly caused by the ethylenic mode of the dark state, has much lower intensity, indicating considerable spectral overlap between the bands of the dark state and of the 123 K photoproduct (the negative band at 1006 cm^{-1}, probably representing the methyl wagging mode of the chromophore, is used for normalization). Therefore, one would also expect considerable overlap between the corresponding visible absorption spectra (see discussion of the time-resolved data) which indeed was found (Chizhov and Engelhard, submitted).

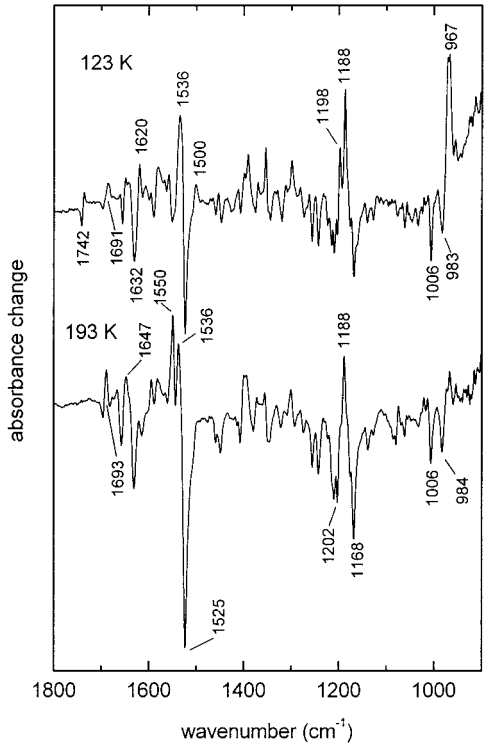

FIGURE 1 Static low-temperature FTIR difference spectra at 123 K (*upper trace*, K state) and; 193 K (*lower trace*, L_1 state). Samples contain ~500 mM chloride. Spectral resolution is 2 cm^{-1}. The negative band at 1525 cm^{-1} of the lower spectrum represents an absorbance change of 1×10^{-2} absorbance units (a.u.).

Congruent with published data for K of sHR (Rothschild et al., 1988), the positive band at 1536 cm^{-1} is interpreted as amide II spectral changes, and the band at 967 cm^{-1}, having strong intensity, is assigned to a hydrogen-out-of-plane mode of the chromophore. The strong intensity indicates a highly twisted chromophore (Fahmy et al., 1989, 1991). In contrast to the K spectrum of bacteriorhodopsin (Siebert and Mäntele, 1983), the fingerprint bands of the dark state between 1260 and 1140 cm^{-1} exhibit considerable fine structure that cannot be explained by different chromophore modes. They represent C—C stretching vibrations coupled to CH bending modes of the chromophore, and, thus, they probably indicate a structural heterogeneous chromophore in the dark state at low temperature. Interestingly, such a heterogeneous chromophore distribution, which is redistributed by illumination and reduced or even abolished at higher temperatures, has also been described for sHR from low-temperature UV-vis spectroscopy (Zimányi et al., 1989). Similarly, this temperature effect is also observed in the spectrum taken at 193 K (Fig. 1, *lower trace*), which displays a considerably reduced fine structure in the fingerprint region of the dark state. It vanishes completely at room temperature (see below). Therefore, it cannot be caused by a possible excitation of the 13-*cis*,15-*syn* chromophore. The 193-K spectrum can be assigned to the low-temperature L_1 state, because it differs from the spectrum obtained at 250 K (Bousché et al., 1991), which has been ascribed to L_2, as reported previously (Chon et al., 1999).

Anions have been shown to influence the bands at 1690 and 1631 cm^{-1} in sHR (Walter and Braiman, 1994). Therefore, we have repeated the measurements of the L_1 state in the presence of 500 mM NaI and 500 mM KBr. A careful analysis with 2 cm^{-1} spectral resolution and zero-filling of

4 did not reveal differences larger than 0.4 cm^{-1} for these two bands, the lower limit being mainly imposed by variations observed among spectra of the same kind. Obviously, these bands seem to be less sensitive in pHR than in sHR-(Braiman et al., 1994;Chon et al., 1999). The 1690 cm^{-1} vibrational mode has been ascribed to a guanidinium mode, tentatively assigned to R123(108) (Braiman et al., 1994; Rüdiger et al., 1995). This interpretation, however, has been questioned because ^2H_2O does not evoke the expected isotope shift (Chon et al., 1999), which is in line with our own observations (not shown).

The other band at 1631 cm^{-1} is located in the region characteristic for the C=N stretching band of the protonated Schiff base in the dark state for both, sHR (Alshuth et al., 1985; Maeda et al., 1985; Pande et al., 1989) and pHR (Gerscher et al., 1997). Also in this case, the anion influence is controversial. Whereas for the C=N stretch in sHR, an anion dependence was described (Maeda et al., 1985; Pande et al., 1989; Walter and Braiman, 1994), which has not been seen in pHR (Gerscher et al., 1997). One has to keep in mind that in the infrared studies the observed anion effects around 1690 and 1631 cm^{-1} may be due to changes of amide I modes that occur in sHR but not in pHR. The C=N stretch of K may be located at 1620 cm^{-1}, and that of L at 1650 cm^{-1}, the latter being approximately in agreement with resonance Raman data. We have found that in L this band is weakly anion dependent (Cl^-: 1650.0 cm^{-1}, Br^-: 1649.1 cm^{-1}, I^-: 1648.5 cm^{-1}, data not shown) in approximate accordance with the resonance Raman results. However, due to the overlap with strong amide I bands, the C=N stretch can only be unequivocally assigned if labeled retinals are used.

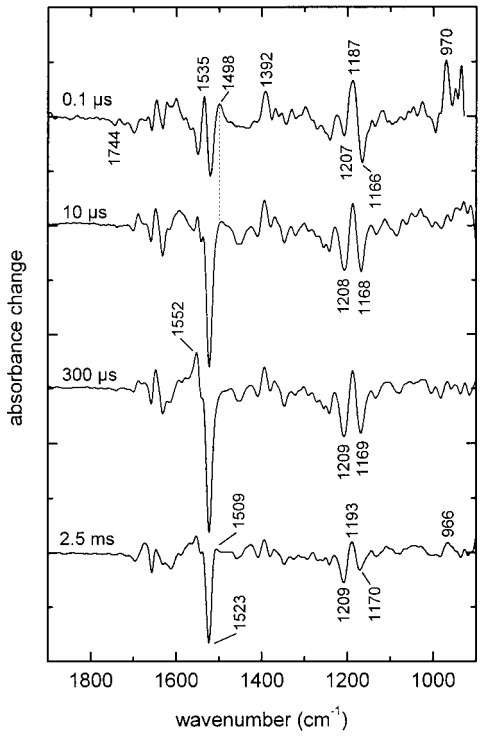

FIGURE 2 Time-resolved step-scan FTIR spectra at selected time slices of pHR containing ~500 mM chloride. The 100-ns spectrum has been obtained with 30-ns time resolution, whereas all the others with 400-ns time resolution. Spectral resolution is 8 cm^{-1}. The negative band at 1525 cm^{-1} of the 10-μs spectrum represents an absorbance change of 1.5×10^{-3} a.u. $T = 300$ K. Bands below 950 cm^{-1} have been omitted due to the increasing noise.

Time-resolved infrared difference spectra (30-ns time resolution and 500 mM NaCl)

The 100-ns spectrum obtained with 30-ns time resolution (Fig. 2) resembles the static K spectrum obtained at 123 K (Fig. 1). The large intensity of the hydrogen-out-of-plane (HOOP) mode at 970 cm^{-1} shows that it is not a property of the low-temperature state, although the position is slightly shifted to higher wavenumbers (all features below 950 cm^{-1} are not further discussed because this spectral range is severely distorted by noise). The bands at 1550 cm^{-1} (negative) and 1536 cm^{-1} (positive) are further common features, although the intensity of the former is much stronger in the time-resolved spectrum. The reduced fine structure of the bands in the finger print region (1140 to 1260 cm^{-1}), as compared to those of the low temperature K spectrum, can only partly be explained by the lower spectral resolutions (8 cm^{-1} *versus* 2 cm^{-1}). As discussed above, the heterogeneity is reduced and finally abolished at higher temperatures. Despite the lower resolution, the two positive bands at 1198 and 1188 cm^{-1} should have been observed in the time-resolved studies. It is interesting to note that the K spectrum of bacteriorhodopsin, in which at low temperature a similar splitting of the positive band is observed, although with different amplitudes, displays a similar sensitivity toward temperature (Siebert and Mäntele, 1983; Weidlich and Siebert, 1993). Apparently, the low temperature imposes slightly different chromophore geometries in the K states of BR as well as of pHR, a conclusion that can also be deduced from the changes of the HOOP modes in both systems. The amide I bands are more intense in the time-resolved than in the static spectrum, indicating larger structural changes. The difference band around 1740 cm^{-1} caused by protonated D156 (141) is less affected.

The analysis of the kinetics obtained with 30-ns time resolution yields only a single half-time of 400 ns, in reasonable agreement with UV-vis data (Váró et al., 1995a) (Chizhov and Engelhard, submitted). Obviously, in this shorter time range the 13-*cis*,15-*syn* retinal conformer in pHR does not contribute to the absorbance changes. Time-resolved step-scan FTIR investigations of sHR have been recently published (Dioumaev and Braiman, 1997). Although many spectral features agree, the reported long life-

time for the K intermediate (360 μs) is clearly in conflict not only with the present data but also with time-resolved UV-vis data of sHR (Váró et al., 1995a).

Time-resolved infrared difference spectra (400-ns time resolution and 500 mM NaCl)

Representative spectra obtained with 400-ns time resolution for times longer than 100 ns are shown in Fig. 2. The complete set of spectra has been analyzed according to the procedure described in Materials and Methods. The global fit reveals four time constants. The corresponding amplitude spectra are presented in Fig. 3. The first time constant of 1.3 μs is considerably affected by the time resolution of the experimental set-up, which only allows to evaluate the data beginning at 1.5 μs. From the amplitude spectra, the spectra of the intermediates have been derived as described in Materials and Methods (Fig. 4.). The first spectrum with the half-time of 1.3 μs is very similar to the 100-ns spectrum of K shown in Fig. 2. However, due to the limited time resolution, it already contains some admixture of L as revealed by the reduced intensities of the HOOP mode at 970 cm^{-1} and of the negative band at 1550 cm^{-1}. The spectrum of the next intermediate (decay time of 57 μs) is

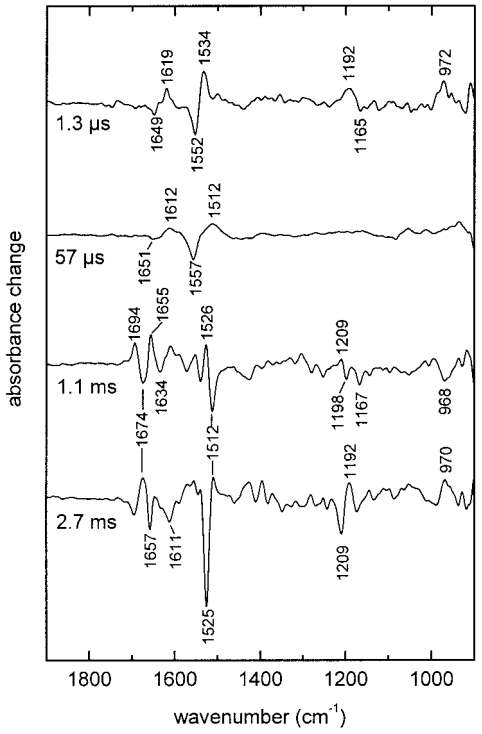

FIGURE 3 Amplitude spectra of the global fit analysis of the time-resolved spectra obtained with 400-ns time resolution, of which selected spectra are shown in Fig. 2. The spectra are labeled according to the half-times of the corresponding exponentials. The negative band at 1512 cm^{-1} in the spectrum, labeled 1.1 ms, corresponds to an absorbance change of 1.4×10^{-3} a.u.

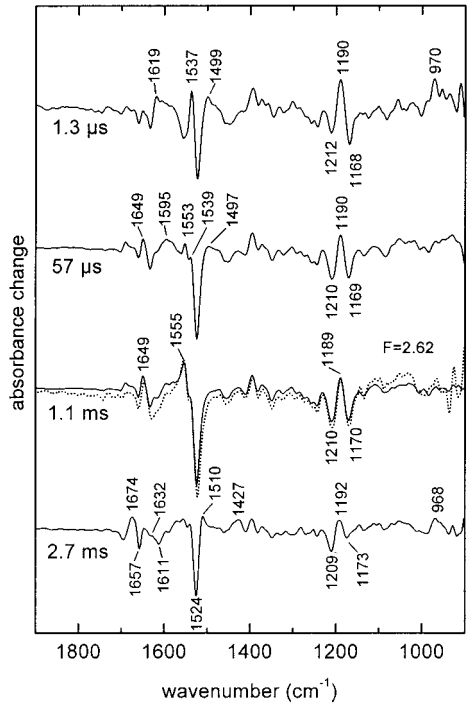

FIGURE 4 Evaluation of the amplitude spectra of Fig. 3 according to the unidirectional reaction model without back-reactions as described in Materials and Methods. The spectra are labeled according to the half-times of the intermediates. The negative band in the 1.3-μs spectrum corresponds to an absorbance change of 2×10^{-3} a.u. Superimposed on the 1.1-ms spectrum (*dotted trace*) is the spectrum obtained from the 2.7-ms spectrum after subtraction of the O content, and subsequent multiplication by a factor of 2.62 for normalization to equal fingerprint band intensities (1210, 1189, and 1170 cm^{-1}).

essentially identical to the spectrum obtained at 10 μs after the flash (Fig. 2). Contributions from the K state are not present any longer, as is evident from the missing HOOP mode. Thus, this spectrum corresponds to a pure L state. This observation is in contrast to the finding of Váró et al. (1995a), who described the presence of ~30% K during the lifetime of the L state. The amplitude spectrum of Fig. 3 (denoted with 1.3 μs) reflects, due to the large separation of the two first time constants, the transition from K to L.

The amplitude spectrum (Fig. 3) with half-time of 57 μs has only bands between 1650 and 1500 cm^{-1} that are very broad. The absence of bands assigned to fingerprint modes excludes that the bands at 1512 and 1557 cm^{-1} originate from ethylenic stretch modes of the chromophore. Instead, all the bands must be assigned to amide I (1612 and 1651 cm^{-1}) and amide II (1557 cm^{-1} and 1512 cm^{-1}) modes. Thus, this transition solely involves changes of the protein and represents, with respect to UV-vis data, a spectrally silent transition.

The resulting intermediate spectrum (half-time, 1.1 ms) is very similar to the previous spectrum. Therefore, the corresponding two species are defined as L_1 (half-time, 57 μ) and

L_2 (half-time, 1.1 ms). In addition to the amide changes discussed, a difference band at 1740 cm^{-1} reappears, although with low amplitude. It is at same position as observed in the K spectra, and is therefore assigned to D156(141). Two L intermediates have also been detected in the photoreaction of sHR using static FTIR difference spectroscopy (Chon et al., 1999). Because of the different species and the different technique, the spectra are difficult to compare.

The following amplitude spectrum (half-time, 2.7 ms) is characterized by intense chromophore as well as protein bands. The large vibrational modes between 1700 and 1600 cm^{-1} mainly reflect changes of amide I bands. The negative band at 1634 cm^{-1} may be assigned to the C=N stretch of the protonated Schiff base of this new intermediate. If so, the positive band at 1652 cm^{-1} would then contain contribution from the C=N stretch of L_2. However, due to the overlap with amide modes, an unequivocal assignment can only be made with isotopically labeled chromophores. The bands in the fingerprint region indicate that the chromophore undergoes alterations. In this time range the rise of the O intermediate, which absorbs above 600 nm, has been reported ((Váró et al., 1995a; Chizhov and Engelhard, submitted; our own control measurements). In agreement with this, the negative band at 1512 cm^{-1} indicates the rise of the ethylenic mode of the red-shifted photoproduct. All the features discussed can also been seen in the intermediate spectrum. The reduced intensity of the fingerprint mode of the dark state at 1169 cm^{-1} (C_{10}—C_{11} stretch) indicates that the chromophore is partially isomerized to the all-*trans* geometry. However, from the comparison with the corresponding spectrum of O of bacteriorhodopsin, a positive band would have been expected around this position (Hessling et al., 1993; Zscherp and Heberle, 1997). Furthermore, the small intensity of the ethylenic mode at 1512 cm^{-1} shows that this intermediate cannot be due only to a red-shifted intermediate, but that it must rather represent a mixture (see below). From the broad feature around 970 cm^{-1} representing several HOOP modes one has to conclude that the chromophore is in a twisted conformation. Whereas all the previous intermediate spectra represent rather pure states, correctly described by the reaction model, this last intermediate spectrum containing a mixture of states is a clear consequence of the adopted linear reaction scheme without back-reactions. The described spectral changes over the complete time range can be nicely followed in the time traces at selected wavenumbers shown in Fig. 5, in which the traces of the global fit are also presented. Due to memory limitations of the transient recorder board, we were unable to follow the photocycle in one single measurement beyond the time range shown. Therefore, we were unable to detect the HR′→ HR reaction with a half time of ~20 ms (Váró et al., 1995a). However, the pronounced decay of all the traces before 10 ms clearly demonstrates that HR′ cannot be very different from HR (the dark state of pHR).

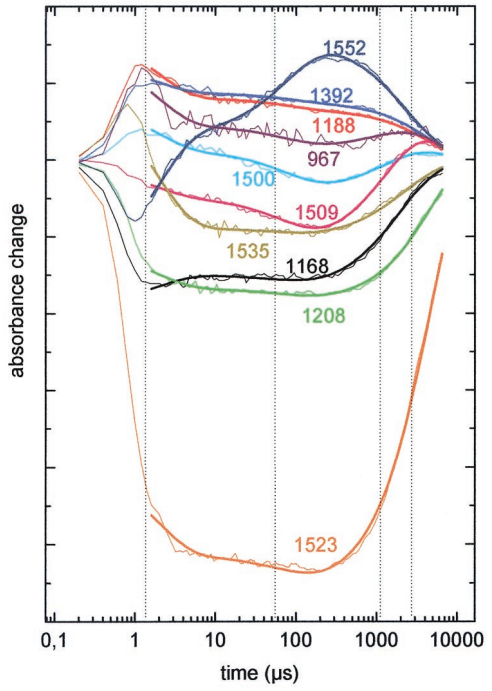

FIGURE 5 Time-traces at selected wavenumbers of the data set evaluated in Figs. 3 and 4. The maximum absorbance change at 1523 cm^{-1} is $-1.8 \times 10 \times -3$ a.u.

Because the first three half times are well separated, the first three intermediate spectra are very similar to the first three time-resolved spectra taken at times before the respective decay has substantially started (Fig. 2).

Time resolved measurements of chloride depleted pHR

In the case of pHR a blue species (pHR^{blue}) with an absorption maximum at 600 nm can be generated by suspending it in distilled water. The original purple state can be regained by the addition of monovalent anions (Scharf and Engelhard, 1994). The red-shift is interpreted by the removal of the counterion from the protonated Schiff base. Surprisingly, the investigation of the photocycle of pHR^{blue} in the infrared was impossible, because the necessary reduction of water for the preparation of the hydrated film samples led to a reconversion of the blue form back into the purple form. The effect is neither caused by residual anions present if an elemental analysis and the binding constant of ~3 mM (Scharf and Engelhard, 1994) are taken into account. Nor can the transition be due to anions dissolved from the infrared window (BaF_2), because the same observation has been made for films on ZnSe or polyethylene support. The blue to purple conversion had already occurred at a quite high water content of the sample, which would not yet allow

infrared measurements. This is different from bacteriorhodopsin, in which the transition occurs at very low water content (Fahmy and Siebert, 1990).

Despite the lack of transportable anions, our control measurements in the UV-vis showed that the photocycle of this anion-depleted hydrated film sample was identical to that in the presence of 10 mM chloride, but not to that of pHR^{blue} in solution. Furthermore, time-resolved infrared measurements at 10 mM NaCL revealed no differences. In the following, the time-resolved infrared spectra of such a hydrated film sample without chloride (denoted "measurement without chloride") are discussed.

Within the signal/noise ratio, the K spectrum obtained with 30-ns time resolution is undistinguishable from the spectrum obtained with 500 mM chloride (not shown). The analysis of the data collected with 400-ns time resolution yielded half-times of 1.6, 48, 1723, and 6249 μs. With the exception of the latter, they compare well with those of the 500-mM measurement. Also, the corresponding amplitude and intermediate spectra reveal no differences within the noise level, and they are, therefore, not reproduced here. The small influence of anions on the band around 1650 cm^{-1} observed at low temperature would not have been detectable in these data. It is important to emphasize that the same spectral features are observed in the $L_1 \rightarrow L_2$ transition, i.e., this transition does not depend on the presence of chloride. However, the amplitude spectrum with half-time of 1.7 ms and the corresponding intermediate spectrum with half time of 6.2 ms are clearly different (Fig. 6). In the amplitude spectrum the larger ethylenic mode at 1511 cm^{-1} indicates that a higher fraction of O is produced. Its real position has to be up-shifted by 3 cm^{-1} due to the overlap with the band of the dark state, and, thus, an absorption maximum between 600 and 610 nm can be deduced using a ratio $\Delta\lambda_{max}/\Delta\nu$ of ~3.5 (Ottolenghi, 1980) and the corresponding values of O of bacteriorhodopsin [λ_{max} 630 nm (Chizhov et al., 1996); C = C stretch: 1509 cm^{-1} (Smith et al., 1983)]. The large amplitude of bands in the amide I region indicate considerable structural changes in the peptide backbone. Both features are equally evident in the intermediate spectrum (compare with 1.1 and 2.7 ms spectra of Fig. 4). The two positive bands in the fingerprint region at 1196 and 1165 cm^{-1} (Fig. 6) clearly demonstrate the all-*trans* geometry of the chromophore in O (Zscherp and Heberle, 1997). The all-*trans* geometry has also been deduced from static FTIR investigations using steady-state illumination at low and high chloride concentration (Váró et al., 1995a). Because of the lower noise in our data, the spectra are difficult to compare. The broad HOOP mode around 964 cm^{-1} and the possible shift of the C=N stretch from 1655 to 1632 cm^{-1} have been already been mentioned in the presentation of the last spectrum of Fig. 4. These bands now have larger amplitudes due to the higher content of O. Indeed, in the intermediate spectrum, the negative band at 1632 cm^{-1} is not present, indicating the total compensation of the band due to the C=N stretch of the dark state by another band of the O intermediate, supporting its identification with the C=N stretch of O.

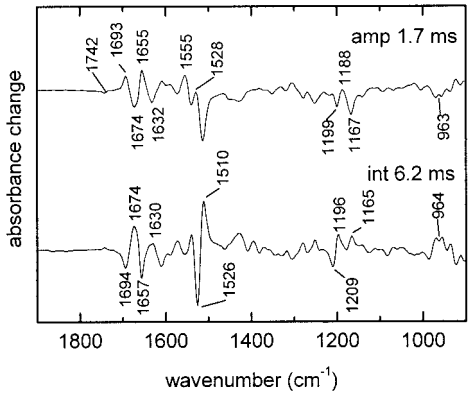

FIGURE 6 Amplitude spectrum of exponential with 1.7-ms half-time and intermediate spectrum with half-time of 6.2 ms of the time-resolved step-scan measurement without chloride. The latter spectrum has been obtained as described in Materials and Methods, and essentially represents the transition to the O state. Its negative band at 1526 cm^{-1} corresponds to an absorbance change of 1.2×10^{-3} a.u. Spectral resolution, 8 cm^{-1}. T = 300 K.

Based on the analysis of time-resolved UV-vis data of pHR at different NaCl concentrations (Chizhov and Engelhard, submitted), the intermediate spectrum (6.2 ms) should essentially represent a pure O state. Therefore it can be used to decompose the 2.7 ms intermediate spectrum of Fig. 4 which does not reflect that of a pure single component. A fraction of the 6.2-ms spectrum (Fig. 6) is subtracted from 2.7-ms spectrum (Fig. 4), compensating the characteristic ethylenic stretch and HOOP modes of O (dashed line in Fig. 4, multiplied by 2.62). The comparison reveals, within the noise limits, no differences from the 1.1-ms spectrum. Obviously, our data show that O is in equilibrium with L_2. An N-like state, as it was described for bacteriorhodopsin could not be identified. The factor of 2.62 (see legend to Fig. 4) indicates that ~62% O are present in the mixture.

Time resolved measurements at high chloride concentration

In order to obtain more information on the chloride transport process, we performed time-resolved infrared measurements at very high chloride concentrations (6 M), at which the chloride release process may be impaired (Bamberg et al., 1984). At high salt concentrations, the infrared transmission of the samples is very poor, resulting in much larger noise in the spectra. The kinetic analysis of the measurements with 400-ns time resolution revealed half-times of 0.4, 61, 955, and 4900 μs (Fig. 7, amplitude spectra (Fig. 8), intermediate spectra). Because of the large noise, we omit the K spectrum. The 61- and 955-μs intermediate spectra very closely resemble those of L_1 and L_2, respectively. Also

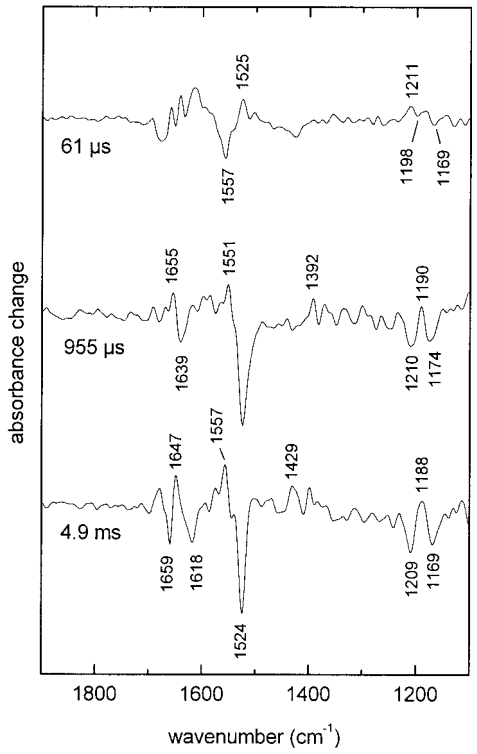

FIGURE 7 Amplitude spectra of the step-scan measurement with halorhodopsin containing ~6 M chloride. The spectra are labeled according to the half-times of the corresponding exponentials. The negative band of the 955-μs spectrum corresponds to an absorbance change of 6.5×10^{-4} a.u. $T = 300$ K. The very first component (0.4 μs) and the spectral region below 1100 cm^{-1} have been omitted because of the poor signal:noise ratio.

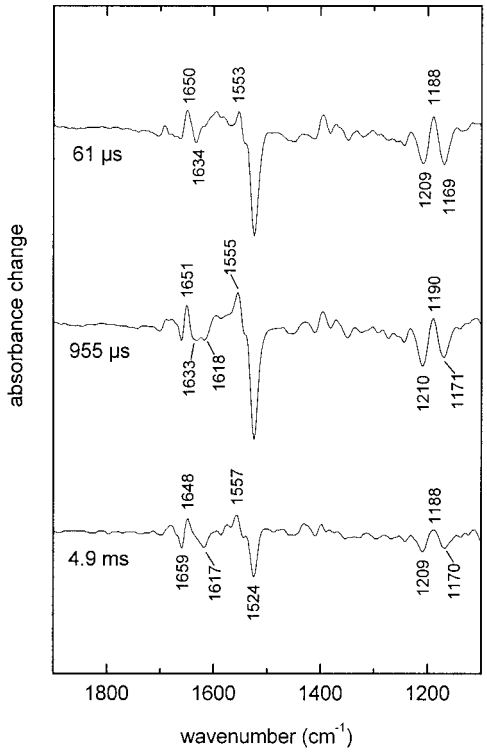

FIGURE 8 Evaluation of the amplitude spectra of Fig. 7 according to the unidirectional model without backreactions as described in Materials and Methods. The negative band of the 955-μs spectrum corresponds to an absorbance change of 1.2×10^{-3} a.u.

the half-times are not drastically changed, with L_2 decaying somewhat faster at very high salt concentration. However, whereas in the $L_1 \rightarrow L_2$ transition at 500 mM chloride or without chloride only protein modes are involved, small contributions of the chromophore can be clearly seen in the fingerprint region at 6 M chloride. Aside from this feature, the corresponding amplitude spectrum, denoted as 61 μs, essentially represents the difference between L_1 and L_2 discussed previously. The bands in the fingerprint region very closely resembles the pattern observed in the $L_2 \rightarrow L_2$/O transition depicted in Fig. 3 (1.1-ms trace). It can be concluded that in the L_2 state at 6 M chloride a small percentage of the chromophore is already back-isomerized to all-*trans*, and that the chromophore geometry in this all-*trans* species must be similar to that of O, i.e., different from that of the dark state. Under these conditions, the O-intermediate itself is not formed because an absorbance increase at 1512 cm^{-1} is absent. Surprisingly, the 955-μs amplitude spectrum represents to a large extent already the decay to the initial state, because it contains most of the negative bands of the intermediate spectra representing the dark state. Consequently, the last intermediate spectrum has a considerable reduced amplitude, but is otherwise very similar to the spectrum of L_2. However, the bands in the amide I region, if normalized to the ethylenic mode at 1524 cm^{-1}, have considerably larger amplitude. Superficially, they resemble the bands observed in O, but a careful comparison reveals clear differences in band position. We call this state L_2'.

DISCUSSION

Characterization of the intermediates

One difficulty in the analysis of the photoreaction of pHR could arise from the partial presence of the 13-*cis*,15-*syn* geometry of the chromophore (10 to 15%) in the dark, as well as in the light-adapted state (Váró et al., 1995a). Flash photolysis experiments comparing sHR and pHR have shown that this species does not contribute to absorbance changes at times longer than 100 ns (Váró et al., 1995a). Therefore, we can also neglect this species in our time-resolved infrared measurements. This is corroborated by the analysis of the data with higher time-resolution, which reveals only one time-constant reflecting the decay to L. Thus, it appears adequate to also ignore this species in the low-temperature spectra.

The low temperature L spectra provide important information on the interaction of anions (chloride, bromide,

iodide) with the protein: 1) the band structure around 1690 cm^{-1} is not influenced by anions in contrast to sHR; 2) no influence of anions can be seen around 1630 cm^{-1} in contrast to sHR, i.e., the C=N stretch of the Schiff base of the dark state is not affected; 3) we tentatively confirm the effect of anions on the C=N stretch of the L state (Gerscher et al., 1997). In principle, the size of the anions should have an influence on the C=N stretching vibration if the binding site is close to the Schiff base. Although the ionic radii of the halides increase from 1.8 Å (Cl^-) to 2.2 Å (I^-), an effect on the C=N-stretch vibrational mode of pHR, in contrast to sHR, has not been observed. Taking the recently published structure of sHR, in which Cl^- is seen in a distance of only 3.8 Å, into account (Kolbe et al., 2000), the binding site of the anion in pHR must be different from that in sHR. Its size is probably larger and/or more flexible to accommodate anions like iodide without affecting the direct Schiff base environment.

Because ^2H_2O causes no change in the band pattern around 1690 cm^{-1}, we agree with earlier conclusions (Chon et al., 1999) that it cannot be caused by R123(108); pHR and sHR show a very similar band pattern, indicating that it has similar molecular origin. This interpretation is in line with the published structure, which indicates only an indirect interaction of the anion with R123(108) via two water molecules. It is not clear which molecular group causes this pattern. However, the lack of anion influence indicates, as compared to sHR, a reduced interaction of the anions with the protein. This observation further corroborates a less restricted binding site. This may explain why pHR, in contrast to sHR, pumps nitrate as effectively as chloride, and, probably, to a small extent, sulfate (Duschl et al., 1990). These differences between pHR and sHR might also be the cause for the observation that pHR, but not sHR, forms a blue membrane.

In the amplitude spectrum reflecting the transition of K to L (1.3 μs), one would expect to observe the ethylenic modes of the chromophore. The C=C stretch of the L-intermediate, having its maximum at 520 nm (Ludmann et al., 2000; Váró et al., 1995a; Chizhov and Engelhard, submitted), could correspond to the band 1552 cm^{-1} and that of K to the low-frequency part of the broad band at 1534 cm^{-1} if, as suggested in Results, an absorption maximum of K close to that of the dark state is assumed. The lack of a positive band at 1512 cm^{-1} excludes an absorption maximum of K close to 600 nm. Thus, this amplitude spectrum also supports an absorption maximum of K around 575 nm, in agreement with Duschl et al. (1990) and Chizhov and Engelhard (submitted).

As expected, the main differences between the spectra of time-resolved L_1 and low-temperature L_1 are caused by the different spectral resolutions and by the fine structure discussed above. Most of the broadened bands can be reproduced by convoluting the bands of the low-temperature spectrum with a broader bandshape. However, the low intensity of the two bands at 1539 and 1553 cm^{-1}, using the bands between 1650 and 1630 cm^{-1} for normalization, cannot be explained in this way. In resonance Raman experiments the C=C stretching mode of L in the presence of chloride (denoted as pHR_{520}) has been located at 1550 cm^{-1} (Gerscher et al., 1997). Because in the infrared amide II modes may also contribute, we can conclude that the time-resolved L state is characterized by an ethylenic stretching mode with very low infrared intensity, similar to the L state of BR (Rödig et al., 1999). Furthermore, the composite character of the band at 1553 cm^{-1} does not allow to identify possible anion-induced shifts as have been described in the resonance Raman experiments. The band at 1536 cm^{-1} also has considerably higher intensity in the low-temperature spectrum and is attributed to an amide II mode. The isomerization of the chromophore in the more rigid protein structure at low temperature probably causes locally larger distortions in the peptide backbone. Thus, at room temperature, the early part of the photocycle exhibits considerably more dynamic behavior than at low temperature: protein changes are larger, but smaller in L.

Measurements in the absence of chloride (or at 10 mM NaCl) allowed us to obtain an essentially pure O spectrum (Fig. 6), an intermediate whose existence has also been proposed from time-resolved UV-vis investigations (Váró et al., 1995a). The spectral properties of this red-shifted intermediate has been explained by canceling the interaction of the Schiff base with the anion. The twisted chromophore geometry deduced from the HOOP modes appears to be a property of intermediates formed after thermal back-isomerization, since similar HOOP modes have also been reported for O of bacteriorhodopsin (Rödig et al., 1999;Smith et al., 1983) and that of the Y185F bacteriorhodopsin mutant (He et al., 1993). Our data clearly show that the chromophore geometry in this intermediate is all-*trans*. Thus, one could speculate that this intermediate is similar to blue pHR obtained by removal of the anion from its extracellular binding site (Scharf and Engelhard, 1994). However, the strong HOOP modes in O, indicating a non-relaxed chromophore, argue against this identity. Attenuated total reflection (ATR)-FTIR titration experiments, which can be performed at higher water content, are in progress to characterize the dark state in the absence of a monovalent anion.

The rise of the pure O state under anion-free conditions is well separated from its precursor L_2. Raising the chloride concentration to 500 mM chloride establishes a fast equilibrium between O and L_2 with a transient concentration of ~60% O (Fig. 4). It is important to emphasize that the spectral properties of this L_2 state are, within the noise level, indistinguishable from the L_2 intermediate determined as a pure state in the time-resolved infrared difference spectra. This observation is in contrast to time-resolved UV-vis studies, which indicate the presence of an N-like species with an, with respect to L, red-shifted absorption maximum

(Váró et al., 1995a). The question arises if these discrepancies concerning the existence of an N intermediate are due to the evaluation method. Generally, a reaction model in which an extra component is introduced would require an additional time constant. However, within the noise level of our data, an additional time-constant does not reduce the error in the global fit and does not improve the sum of residuals. This shows that, if indeed an N state is present, its spectral properties must be very similar to those of the L_2 state, which is in contrast to the above cited UV-vis analysis. Recent time-resolved UV-vis investigations show the presence of an N state that, however, has an absorption maximum indistinguishable from that of L (Chizhov and Engelhard, submitted). The identification of transitions that are spectrally silent also in the infrared requires very high signal/noise ratio. Nevertheless, although there are some deviations in details of the reaction models, all assume that the O state, which has an all-*trans* chromophore, is in equilibrium with a species with a 13-*cis* isomer.

At present we can only speculate why the anion-free form of the hydrated film samples displays spectral properties and a photocycle identical to that of pHR at 10 mM NaCl. Although the anion-free form of sHR in solution displays an absorption maximum at 570 nm, i.e., even little blue-shifted from the chloride-bound form, the photocycle is completely different (Oesterhelt, 1995). Therefore, the two systems cannot be compared. The absorption maximum in the chloride-free infrared sample around 578 nm requires the presence of a counterion, substituting for the chloride. Sulfate, which is present in our sample (originating from the Tris/H_2SO_4 buffer), cannot be involved because the same transformation from the blue to the purple also occurs if distilled water is used. Also, a simple concentration increase of any negatively charged species seems unlikely, because otherwise it should have also been possible to induce the purple form in suspensions of pHR without a transportable anion. The possibility that a residue of halorhodopsin itself takes over the function of the counterion (e.g., D252(238) by movement of R123(108) toward the extracellular side) can be excluded because the photocycle should be considerably different from that involving an active anion transport. A likely explanation could be that the close neighborhood of adjacent membranes in the hydrated films induces alterations in the anion binding site, such that an OH^- ion substitutes for chloride even at pH 7. Further experiments are required to explain the absorption maximum and the photocycle kinetics of the chloride-free hydrated film samples. However, irrespective of the mechanism, the time-resolved infrared studies of the chloride-free samples confirm that the anions have very little influence on the spectra.

At 6 M NaCl, the photocycle is drastically changed. 1) With the formation of L_2 the chromophore is already partially backisomerized to all-*trans*, the corresponding chromophore geometry being similar to that of O but different from that of the dark state. 2) An intermediate is formed that is different both from this L_2 and different from O, and because of its greater similarity to L_2 we have termed it L_2'. A further peculiarity of this intermediate is the small amplitude of negative chromophore bands, demonstrating that a considerable fraction of L_2 has already decayed to the initial state with the formation of L_2'. If the unidirectional reaction scheme would be applied for this transition, this would show that L_2' is in equilibrium with the dark state. Because this putative equilibrium is completely transformed into the dark state with the last step, i.e., irreversibly, we regard this interpretation as unlikely. Of course, we cannot exclude that the putative equilibrium does not contain the dark state, but a state very similar to that, and that the irreversible transition is from this pseudo-dark state to the dark state. However, it is difficult to reconcile an irreversible step between two species differing very little in their molecular properties as determined by infrared spectroscopy.

As an alternative, we propose a branching of the reaction cycle at the L_2 state, according to the following scheme:

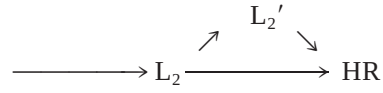

Neglecting the fast formation of L_2, the kinetic analysis shows that two rate constants, k_1 and k_2, describe this scheme, whereby $k_1 = k_{LL'} + k_{LHR}$ and $k_2 = k_{L'HR}$ ($k_{LL'}$, k_{LHR}, and $k_{L'HR}$ being the microscopic rate constants for the decay of L_2 to L_2', L_2 to HR, and of L_2' to HR, respectively. Thus, the amplitude spectrum with the half-time of 4.9 ms describes the decay of the L_2' as assumed (Figs. 7 and 8), whereas the amplitude spectrum with half-time of 955 μs contains contributions of the intermediate L_2 and L_2'. Using the fact that the rise of L_2 is much faster than its decay, the intermediate spectrum of L_2 is essentially given by the sum of the last two amplitude spectra shown in Fig. 7. As in the case of the unidirectional model, the last intermediate spectrum of the branched model is given by the last amplitude spectrum. However, the scaling is different. Whereas in the sequential model, the amplitude spectrum is multiplied by $(k_{LL'} + k_{LHR} - k_{L'HR})/(k_{LL'} + k_{LHR})$, using the rate constants of the branched model, in the branched model it is multiplied by $(k_{LL'} + k_{LHR} + k_{L'HR})/k_{L'HR}$. The former factor amounts to 0.86, explaining the reduced amplitude in Fig. 8, whereas the latter factor has the higher value of 6.1. The large factor is due to the model in which the spectrum is scaled as if all cycling molecules would pass via L_2. Therefore, the observed amplitude and intermediate spectra of Fig. 7 and 8 can be well explained by the branched reaction model.

Consequences for the anion transport mechanism

The structure of sHR has clearly demonstrated the chloride binding site in the dark state to be on the extra-cellelular side from the Schiff base (Kolbe et al., 2000), and it can be expected that this applies also to pHR, although the binding site appears less restricted. The formation of the L_1-intermediate is accompanied by an approach of the anion toward the Schiff base, which had already been concluded from the resonance Raman experiments and is now confirmed by our infrared data. Once this movement has happened, the protein undergoes a conformational change that only involves amide bonds, but not the chromophore, thereby forming the intermediate L_2. With respect to time-resolved UV-vis measurements, this transition is spectrally silent and only kinetically apparent as demonstrated for sHR (Váró et al., 1995c) and pHR (Ludmann et al., 2000; Chizhov and Engelhard, submitted).

Because the conformational changes between L_1 and L_2 are larger than those between L_2 and a putative N state, the former transition might reflect the accessibility change of the anion from the extracellular side in L_1 to the cytosolic side in L_2. A similar interpretation for the two L states has been put forward for sHR (Kolbe et al., 2000), whereas for pHR the change in accessibility has been connected to the L $\rightarrow$ N transition (Ludmann et al., 2000). However, in view of our different results on the N state, this conclusion may be questionable. The larger amide I changes observed for the O state could reflect the alteration of the binding constant and/or the opening of the channel, enabling the transport of the anion from a site still close to the Schiff base to the cytosolic membrane surface or aqueous phase. In line with this interpretation is the observation that, for pHR, a large electrogenicity is connected with the formation of O (Ludmann et al., 2000). If this view is accepted, the decay of O must involve more molecular events than the mere binding of the anion from the extracellular side. Before this can happen, a switch that restores the original accessibility has to occur. It is possible that the switch has already taken place in O. The observed L_2/O equilibrium does not contradict this proposal, because an equilibrium between states of different accessibilities is also observed in bacteriorhodopsin (either L/M_2 or M/N). It could, however, also occur in a different O state with altered protein conformation, which, however, is not accumulated due to rapid chloride uptake, but was proposed by Chizhov and Engelhard (submitted). Time-resolved ATR-FTIR investigations may provide further information about such an additional protein state.

We observed an acceleration of the decay of the L/O equilibrium with increasing chloride concentration (5.9 ms at 50 mM, 3.5 ms at 250 mM, and 2.7 ms at 500 mM). A chloride-dependent rate constant from O to HR′ has also been deduced from time-resolved UV-vis measurements (Váró et al., 1995a). One could think that this anion dependence is caused by a rate determined by the recombination with chloride. However, the half-time of 6.2 ms obtained in measurements without chloride is clearly not in agreement with such a fast rate. Here, some other mechanism must restore the initial state.

How can the branching model be incorporated in the anion transport mechanism? As already mentioned, high chloride concentrations (6 M, close to saturation) inhibit the transfer of the anion from the site it occupies in L_2 (still close to the Schiff base) to the release site (probably close to the cytosolic surface). The branching will become apparent once the decay of L_2 via the L_2/O equilibrium is slowed down due to the strongly reduced partitioning of O in the equilibrium. Our own data and recent time-resolved UV-vis measurements (Chizhov and Engelhard, submitted) at varying chloride concentrations demonstrate that in the 0.1- to 2-M concentration range the O amplitude in the equilibrium is strongly dependent on the concentration, and a binding constant of 1 M has been deduced. At saturating NaCl concentration, hardly any O would be observed. It appears that, if the slowing down via the L_2/O pathway occurs, the protein can relax via two different pathways, resulting in the branching. The direct relaxation from L_2 to HR represents a shortcut in the anion transport mechanism. The anion would be transferred from the L_2 site back to the initial binding site. The functional consequence of the other path, leading via L_2' to the dark state, is less clear. The spectra of Fig. 8 demonstrate that the chromophore geometry in both L_2 and $L_2'$are indistinguishable, i.e., a fraction of both contain already an all-*trans* chromophore. The high anion concentration could cause protonation of the uptake site, although the chromophore is still largely 13-*cis*. The simultaneous occupation of this site, of the site in L_2, and of the release site could cause the large amide changes in L_2'. This path would probably lead to netto-anion translocation, because in the transition to the dark state the anion at the site of L_2 would finally expel the anion from the release site, due to the fact that the extracellular site with higher affinity in the dark is occupied. The required back-isomerization, either from the L_2 or the L_2' states without passing via the O intermediate, could be facilitated by the partial all-*trans* geometry. We can only speculate about the molecular origin of the altered photoreaction at high NaCl concentration. As suggested by one reviewer, Hofmeister salt effects could play a role. Indeed, as has been shown for bacteriorhodopsin (Dér and Ramsden, 1998) and rhodopsin (Vogel et al., 2001), the protein structure also of membrane proteins can be destabilized by high salt concentrations, thereby influencing the photoreaction. Time-resolved infrared experiments on halorhodopsin using strong chaotropic anions, such as thiocyanate, in addition to the transportable anions could test this hypothesis.

It has been shown that high chloride concentration causes an inhibition of chloride transport, which has been ex-

plained by the occupancy of the release site. (Bamberg et al., 1984; Okuno et al., 1999). In the branching model described here, the inhibition of anion transport is caused by the shortcut of the photocycle from the L_2 directly to the dark state. If a photocycle that always passes through O is assumed, the high chloride concentration would slow down the photocycle, due to the fact that hardly any O could be formed transiently. The observation of normal millisecond kinetics at saturating chloride concentrations requires a photocycle that does not involve O. Therefore, part of the back-reaction occurs from the L_2 state, which results in no netto-transport. The other branch, via L_2', describes a more complicated situation, as it appears possible that ion transport takes place here. It should be emphasized that the spectra of Figs. 7 and 8 are difficult to interpret without branching at L_2. However, further experiments using the ATR method (Heberle and Zscherp, 1996), allowing time-resolved measurements under well-defined salt concentrations, are necessary to corroborate these interpretations.

Outlook

It appears important to further investigate the differences between sHR and pHR in relation to their specific amino acid sequences. The correlation of the fine tuning of their properties with the respective structures will lead to a better understanding of these light-driven anion pumps. The observation that the single-atomic anions influence the infrared spectra very little indicates that the anion-protein interaction does not involve the polar residues that have strong infrared intensity. For the binding site in the dark state, this is in agreement with the published structure of sHR. It will be interesting to see whether nitrate also has such a small influence on the spectra. Corresponding investigations are in progress.

The branching model might be important for the transport against a higher membrane potential as it has been studied in the case of bacteriorhodopsin (Nagel et al., 1998). It remains to be seen if the membrane potential affects the futile chloride cycle in which the anion is picked up and released from the same side. Whereas up to now infrared measurements can only be performed under zero voltage conditions, it certainly would be of great interest to understand the mechanism of chloride transport under more physiological conditions.

We thank R. Müller for technical help and A. A. Wegener for pHR expressed in *E. Coli*. This work was supported by the Deutsche Forschungsgemeinschaft, grant SI 278/18–1,2, and by Fonds der Chemischen Industrie (to F.S.).

REFERENCES

Alshuth, T., M. Stockburger, P. Hegemann, and D. Oesterhelt. 1985. Structure of the retinal chromophore in halorhodopsin: a resonance Raman study. *FEBS Lett.* 179:55–59.

Ames, J. B., J. Raap, J. Lugtenburg, and R. A. Mathies. 1992. Resonance Raman study of halorhodopsin photocycle kinetics, chromophore structure, and chloride-pumping mechanism. *Biochemistry.* 31:12546–12554.

Bamberg, E., P. Hegemann, and D. Oesterhelt. 1984. Reconstitution of the light-driven electrogenic ion pump halorhodopsin in black lipid membranes. *Biochim. Biophys. Acta.* 773:53–60.

Bamberg, E., J. Tittor, and D. Oesterhelt. 1993. Light-driven proton or chloride pumping by halorhodopsin. *Proc. Natl. Acad. Sci. U.S.A.* 90: 639–643.

Bousché, O., E. N. Spudich, J. L. Spudich, and K. J. Rothschild. 1991. Conformational changes in sensory rhodopsin I: similarities and differences with bacteriorhodopsin, halorhodopsin, and rhodopsin. *Biochemistry.* 30:5395–5400.

Braiman, M. S., T. J. Walter, and D. M. Briercheck. 1994. Infrared spectroscopic detection of light-induced change in chloride-arginine interaction in halorhodopsin. *Biochemistry.* 33:1629–1635.

Brown, L. S., A. K. Dioumaev, R. Needleman, and J. K. Lanyi. 1998. Local access model for proton transfer in bacteriorhodopsin. *Biochemistry.* 37:3982–3993.

Chizhov, IV, D. S. Chernavskii, M. Engelhard, K.-H. Müller, B. V. Zubov, and B. Hess. 1996. Spectrally silent transitions in the bacteriorhodopsin photocycle. *Biophys. J.* 71:2329–2345.

Chon, Y.-S., H. Kandori, J. Sasaki, J. K. Lanyi, R. Needleman, and A. Maeda. 1999. Existence of two L photointermediates of halorhodopsin from *Halobacterium salinarium*, differing in their protein and water IR bands. *Biochemistry.* 38:9449–9455.

Dér, A. and J. J. Ramsden. 1998. Evidence for loosening of a protein mechanism. *Naturwissenschaften.* 85:353–355.

Diller, R., M. Stockburger, D. Oesterhelt, and J. Tittor. 1987. Resonance Raman study of intermediates of the halorhodopsin photocycle. *FEBS Lett.* 217:297–304.

Dioumaev, A. K. and M. S. Braiman. 1997. Nano- and microsecond time-resolved FTIR spectroscopy of the halorhodopsin photocycle. *Photochem. Photobiol.* 66:755–763.

Duschl, A., J. K. Lanyi, and L. Zimányi. 1990. Properties and photochemistry of a halorhodopsin from the haloalkaliphile, *Natronobacterium pharaonis*. *J. Biol. Chem.* 265:1261–1267.

Fahmy, K., M. F. Grossjean, F. Siebert, and P. Tavan. 1989. The photoisomerization in bacteriorhodopsin studied by FTIR linear dichroism and photoselection experiments combined with quantumchemical theoretical analysis. *J. Mol. Struct.* 214:257–288.

Fahmy, K. and F. Siebert. 1990. The photoreaction of the deionized form of the purple membrane investigated by FTIR difference spectroscopy. *Photochem. Photobiol.* 51:459–464.

Fahmy, K., F. Siebert, and P. Tavan. 1991. Structural investigation of bacteriorhodopsin and some of its photoproducts by polarized Fourier transform infrared spectroscopic methods: difference spectroscopy and photoselection. *Biophys. J.* 60:989–1001.

Fodor, S. P. A., W. T. Pollard, R. Gebhard, E. M. M. van den Berg, J. Lugtenburg, and R. A. Mathies. 1988. Bacteriorhodopsin's L_{550} intermediate contains a C14–C15 s-*trans*-retinal chromophore. *Proc. Natl. Acad. Sci. U.S.A.* 85:2156–2160.

Gerscher, S., M. Mylrajan, P. Hildebrandt, M.-H. Baron, R. Müller, and M. Engelhard. 1997. Chromophore-anion interaction in halorhodopsin from *Natronobacterium pharaonis* probed by time-resolved resonance Raman spectroscopy. *Biochemistry.* 36:11012–11020.

Gerwert, K. and F. Siebert. 1986. Evidence for light-induced 13-cis, 14-s-cis isomerization in bacteriorhodopsin obtained by FTIR difference spectroscopy using isotopically labelled retinals. *EMBO J.* 5:805–811.

Haupts, U., J. Tittor, E. Bamberg, and D. Oesterhelt. 1997. General concept for ion translocation by halobacterial retinal proteins—the isomerization/switch/transfer (IST) model. *Biochemistry.* 36:2–7.

He, Y., M. P. Krebs, W. B. Fischer, H. G. Khorana, and K. J. Rothschild. 1993. FTIR difference spectroscopy of the bacteriorhodopsin mutant Tyr-185→Phe: detection of a stable O-like species and characterization of its photocycle at low temperature. *Biochemistry.* 32:2282–2290.

Heberle, J. and C. Zscherp. 1996. ATR/FT-IR difference spectroscopy of biological matter with microsecond time resolution. *Appl. Spectrosc.* 50:588–596.

Hessling, B., G. Souvignier, and K. Gerwert. 1993. A model-independent approach to assigning bacteriorhodopsin's intramolecular reactions to photocycle intermediates. *Biophys. J.* 65:1929–1941.

Heyde, M. E., D. Gill, R. G. Kilponen, and L. Rimai. 1971. Raman spectra of Schiff bases of retinal models of visual photoreceptors. *J. Am. Chem. Soc.* 93:6776–6780.

Hohenfeld, I. P., A. A. Wegener, and M. Engelhard. 1999. Purification of histidine tagged bacteriorhodopsin, *pharaonis* halorhodopsin, and *pharaonis* sensory rhodopsin II functionally expressed in *Escherichia coli*. *FEBS Lett.* 442:198–202.

Kalaidzidis, IV, Y. L. Kalaidzidis, and A. D. Kaulen. 1998. Flash-induced voltage changes in halorhodopsin from *Natronobacterium pharaonis*. *FEBS Lett.* 427:59–63.

Kolbe, M., H. Besir, L. O. Essen, and D. Oesterhelt. 2000. Structure of the light-driven chloride pump halorhodopsin at 1.8 Å resolution. *Science.* 288:1390–1396.

Lanyi, J. K., A. Duschl, G. W. Hatfield, K. May, and D. Oesterhelt. 1990. The primary structure of a halorhodopsin from *Natronobacterium pharaonis*. *J. Biol. Chem.* 265:1253–1260.

Losi, A., A. A. Wegener, M. Engelhard, W. Gärtner, and S. E. Braslavsky. 1999. Time-resolved absorption and photothermal measurements with recombinant sensory rhodopsin II from *Natronobacterium pharaonis*. *Biophys. J.* 77:3277–3286.

Ludmann, K., G. Ibron, J. K. Lanyi, and G. Váró. 2000. Charge motions during the photocycle of *pharaonis* halorhodopsin. *Biophys. J.* 78: 959–966.

Maeda, A., T. Ogurusu, T. Yoshizawa, and T. Kitagawa. 1985. Resonance raman study on binding of chloride to the chromophore of halorhodopsin. *Biochemistry.* 24:2517–2521.

Mukohata, Y., K. Ihara, T. Tamura, and Y. Sugiyama. 1999. Halobacterial rhodopsins. *J. Biochem.* 125:649–657.

Müller, K.-H. and Th. Plesser. 1991. Variance reduction by simultaneous multi-exponential analysis of data sets from different experiments. *Eur. Biophys. J.* 19:231–240.

Nagel, G., B. Kelety, B. Möckel, G. Büldt, and E. Bamberg. 1998. Voltage dependence of proton pumping by bacteriorhodopsin is regulated by voltage-sensitive ratio of M_1 to M_2. *Biophys. J.* 74:403–412.

Oesterhelt, D. 1995. Structure and function of halorhodopsin. *Israel J. Chem.* 35:475–494.

Okuno, D., M. Asaumi, and E. Muneyuki. 1999. Chloride concentration dependency of the electrogenic activity of halorhodopsin. *Biochemistry.* 38:5422–5429.

Ottolenghi, M. 1980. The photochemistry of rhodopsin. *In* Advances in Photochemistry, Vol. 12: J.N.Pitts, G.S.Hammond, K.Gollnik, and D.Grosjean, editors. Wiley-Interscience, New York. 97–200.

Pande, C., J. K. Lanyi, and R. H. Callender. 1989. Effects of various anions on the Raman spectrum of halorhodopsin. *Biophys. J.* 55:425–431.

Rothschild, K. J., O. Bousché, M. S. Braiman, C. A. Hasselbacher, and J. L. Spudich. 1988. Fourier transform infrared study of the halorhodopsin chloride pump. *Biochemistry.* 27:2420–2424.

Rödig, C., IV Chizhov, O. Weidlich, and F. Siebert. 1999. Time-resolved step-scan FTIR spectroscopy reveals differences between early and late M intermediates of bacteriorhodopsin. *Biophys. J.* 76:2687–2701.

Rüdiger, M., U. Haupts, K. Gerwert, and D. Oesterhelt. 1995. Chemical reconstitution of a chloride pump inactivated by a single point mutation. *EMBO J.* 14:1599–1606.

Sasaki, J., L. S. Brown, Y.-S. Chon, H. Kandori, A. Maeda, R. Needleman, and J. K. Lanyi. 1995. Conversion of bacteriorhodopsin into a chloride ion pump. *Science.* 269:73–75.

Scharf, B. and M. Engelhard. 1994. Blue halorhodopsin from *Natronobacterium pharaonis*: wavelength regulation by anions. *Biochemistry.* 33: 6387–6393.

Siebert, F. and W. Mäntele. 1983. Investigation of the primary photochemistry of bacteriorhodopsin by low-temperature Fourier-transform infrared spectroscopy. *Eur. J. Biochem.* 130:565–573.

Smith, S. O., J. Lugtenburg, and R. A. Mathies. 1985. Determination of chromophore structure in bacteriorhodopsin with resonance Raman spectroscopy. *J. Membr. Biol.* 85:95.

Smith, S. O., J. A. Pardoen, P. P. J. Mulder, B. Curry, J. Lugtenburg, and R. A. Mathies. 1983. Chromophore structure in bacteriorhodopsin's O_{640} photointermediate. *Biochemistry.* 22:6141–6148.

Tittor, J., U. Haupts, C. Haupts, D. Oesterhelt, A. Becker, and E. Bamberg. 1997. Chloride and proton transport in bacteriorhodopsin mutant D85T: different modes of ion translocation in a retinal protein. *J. Mol. Biol.* 271:405–416.

Uhmann, W., A. Becker, Ch. Taran, and F. Siebert. 1991. Time-resolved FT-IR absorption spectroscopy using a step-scan interferometer. *Appl. Spectrosc.* 45:390–397.

Váró, G., L. S. Brown, R. Needleman, and J. K. Lanyi. 1996. Proton transport by halorhodopsin. *Biochemistry.* 35:6604–6611.

Váró, G., L. S. Brown, J. Sasaki, H. Kandori, A. Maeda, R. Needleman, and J. K. Lanyi. 1995a. Light-driven chloride transport by halorhodopsin from *Natronobacterium pharaonis*. 1. The photochemical cycle. *Biochemistry.* 34:14490–14499.

Váró, G., R. Needleman, and J. K. Lanyi. 1995b. Light-driven chloride transport by halorhodopsin from *Natronobacterium pharaonis*. 2. Chloride release an uptake, protein conformation change, and thermodynamics. *Biochemistry.* 34:14500–14507.

Váró, G., L. Zimányi, X. Fan, L. Sun, R. Needleman, and J. K. Lanyi. 1995c. Photocycle of halorhodopsin from *Halobacterium salinarium*. *Biophys. J.* 68:2062–2072.

Vogel, R., G.-B. Fan, M. Sheves, and F. Siebert. 2001. Salt dependence of the formation and stability of the signaling state in G protein-coupled receptors: evidence for the involvement of the Hofmeister effect. *Biochemistry.* 40:483–493.

Walter, T. J. and M. S. Braiman. 1994. Anion-protein interaction during halorhodopsin pumping: halide binding at the protonated Schiff base. *Biochemistry.* 33:1724–1733.

Weidlich, O. and F. Siebert. 1993. Time-resolved step-scan FT-IR investigations of the transition from KL to L in the bacteriorhodopsin photocycle: identification of chromophore twists by assigning hydrogen-out-of-plane (HOOP) bending vibrations. *Appl. Spectrosc.* 47: 1394–1400.

Zimányi, L. and J. K. Lanyi. 1997. Fourier transform Raman study of retinal isomeric composition and equilibration in halorhodopsin. *J. Phys. Chem. B* 101:1930–1933.

Zimányi, L., P. Ormos, and J. K. Lanyi. 1989. Low-temperature photoreactions of halorhodopsin. 1. Detection of conformational substates of the chromoprotein. *Biochemistry.* 28:1656–1661.

Zscherp, C. and J. Heberle. 1997. Infrared difference spectra of the intermediates L, M, N, and O of the bacteriorhodopsin photoreaction obtained by time-resolved attenuated total reflection spectroscopy. *J. Phys. Chem. B.* 101:10542–10547.